Research Article

Hiba Jameel Alabedi* and Saleh Issa Khassaf

Numerical study on discharge capacity of piano key side weir with various ratios of the crest length to the width

https://doi.org/10.1515/eng-2022-0536
received July 12, 2023; accepted September 05, 2023

Abstract: A side or lateral weir can be defined as a longitudinal weir put in parallel to the main flow direction. A piano key side weir (PKSW) is one of the various side weirs used to control flow level, flow diversion, and flood harm prevention in dams and hydraulic systems. A side weir aims to keep the water level in the main channel at a specific level by discharging the overflow water into a side channel. The discharge coefficient of the PKSW was covered in this study by numerical modeling of a rectangular PKSW type B with various ratios of the crest length to the width in a straight channel. Results showed that the discharge coefficient of the PKSW was more affected by the L/W parameter when the other parameters were constant. It was noted that the PKSW discharge coefficient for L/W equal to 6 demonstrated a significantly higher level of performance and also found that increasing the upstream head above the side weir crest (h_a/P) negatively affected the coefficient of discharge. It was concluded that a high capacity of the discharge coefficient required the (h_a/P) ratio to be smaller than 0.75 or within the range ($0.3 \le h_a/P < 0.75$).

Keywords: piano key side weir, numerical modeling, the discharge coefficient, flow-3D software

1 Introduction

A piano key weir (PKW) is a particular type of labyrinth that is used to increase the discharge capacity in the low head in the main channel, while a piano key side weir (PKSW) is a type of side weir that is put in parallel to the main flow direction, i.e., it is placed in the side of the main channel with a specific angle. The PKSW is defined as a non-linear weir and has a discharge greater than that of a linear weir due to expanding in length and width. The basic geometry structure of PKSW is the same as PKW but it is not the same in a location. The objective of a PKSW is to keep the water level in the main channel at a specific level by discharging the overflow water into a side channel. It is often used in irrigation techniques, wastewater networks, and flood prevention precautions. The PKW is a modern kind of nonlinear control structure with a relatively small slope spillway.

The standard design model of the PKW is not available, and there are large numbers of geometric parameters affecting the head-discharge performance of the PKSW [1]. Large attention is given to PKWs as a type of dam because of flood control, drinking water requirements, and the ability to power hydroelectric and irrigation [2]. The formative shape of PKW is a simple rectangular layout; therefore, the figuration of a rectangular styling is identical to the keys of a piano, and from this similarity, the PKW was named. The zigzag shape of PKW supplies further length that leads to a rise in the discharge capacity without a rise in the zone of submergence of upstream of the dam. The construction of the PKW becomes easier because of the rectangular layout by using precast units [3].

In 1998, the prefatory studies of PKW began by the non-governmental organization “Hydrocoop” (France); however, the final design was not yet agreed upon, but the major principle of overhangs was included. Improvements and research were then performed in collaboration with the Biskra University (Algeria) till a basic paper about the subject was published in 2003 by F. Lempérière (from Hydrocoop) and A. Ouamane (from Biskra) to simplify and improve the performance of labyrinth-type weirs installed on the smaller spillway footprints. Since 2003, hundreds of studies have been implemented in France, Algeria, India, China, and Vietnam [4]. All these studies

*** Corresponding author: Hiba Jameel Alabedi,** Department of Civil Engineering, College of Engineering, University of Basrah, Center of Basrah, PO Box 49, Al Basrah, Iraq, e-mail: hibajameel.m@gmail.com
Saleh Issa Khassaf: Department of Civil Engineering, College of Engineering, University of Basrah, Center of Basrah, PO Box 49, Al Basrah, Iraq, e-mail: saleh.khassaf@uobasrah.edu.iq

and research had the same practical goals. Depending on the layout model of overhangs in the upstream and downstream, there are four types of PKW (A, B, C, and D) suggested by Lempérière et al. [4] as shown in Figure 1.

There is a large set of geometric parameters that are included in PKW geometry, it seems as an assemblage of several elements [6] as shown in Figure 2.

There are relatively limited studies on PKSWs in the literature. One of the first studies to examine PKSW was conducted by Karimi et al. [7]. They studied the investigation and comparison of the free surface flow properties over PKSWs type C, rectangular labyrinth side weirs (RLSWs), and labyrinth side weirs (LSWs) in the straight channel. Results showed that PKSW and LSWs were more effective than equivalent linear side weirs. Mehri et al. [8] evaluated and analyzed a discharge coefficient of a PKSW type C, with specific descriptions at 30° and 120° portions of a channel with a longitudinal curvature. They found that both the discharge coefficient at 30° and 120° angles were influenced by the parameter P/h_1 of the PKSW, which increases with the increase in the discharge coefficient value. Seyedjavad et al. [9] studied the trapezoidal PKSW (TPKSW) type A in the straight channel. In this study, an empirical equation was used to calculate the coefficient of discharge of (TPKSW) type A. Also, Saghari et al. [10] focused on the impact of employing one or two cycles in the TPKSWs type A on the discharge coefficient at bend curvatures of 60°, 105°, and 150°, and the intake channels were orthogonal to the main channel. The study found that the C_{dL} of the TPKSWs with one cycle was 1.4–2 times greater than that of the TPKSWs with two cycles. Karimi et al. [11] examined how the PKSWs performed through various key angles in the lab and with the use of Computational Fluid Dynamics (CFD) modeling.

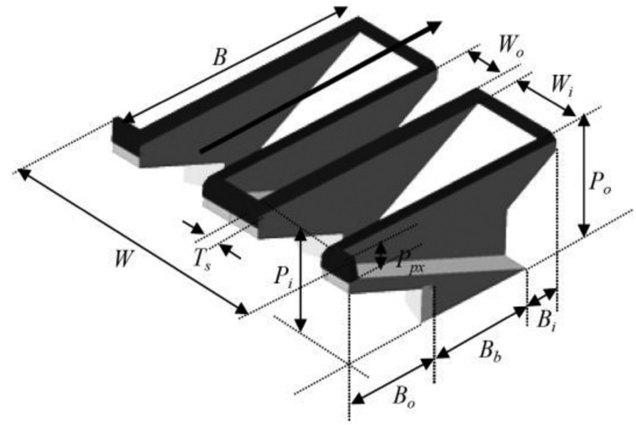

Figure 2: Major parameters of PKW in three-dimensional view [6].

The results showed that the PKSW 30° has a higher discharge coefficient (C_d) than the PKSW with other angles. Mehri et al. [12] compared the discharge coefficient of rectangular PKSWs (RPKSWs) with four types (A, B, C, and D) in the curved channel. The results show that, proposed an equation for each of A, B, C, and D type, and the P/h_1 ratio was the most effective parameter on the coefficient of discharge for all types of PKSWs. It was also found that the hydraulic performance of B type RPKSW was superior to that of other types at 120°. Kilic and Emiroglu [13] conducted an experimental investigation on the hydraulic properties of the TPKSW in straight channels, and evaluated the suitability of the De Marchi, Dominguez, and Schmidt methods by comparing the results obtained for TPKSW and generating a useful and reliable equation for TPKSW. The results showed that the discharge coefficient rose when the P/W ratio declined.

In the current study, a CFD technique by the Flow-3D software was utilized to simulate the hydraulic properties

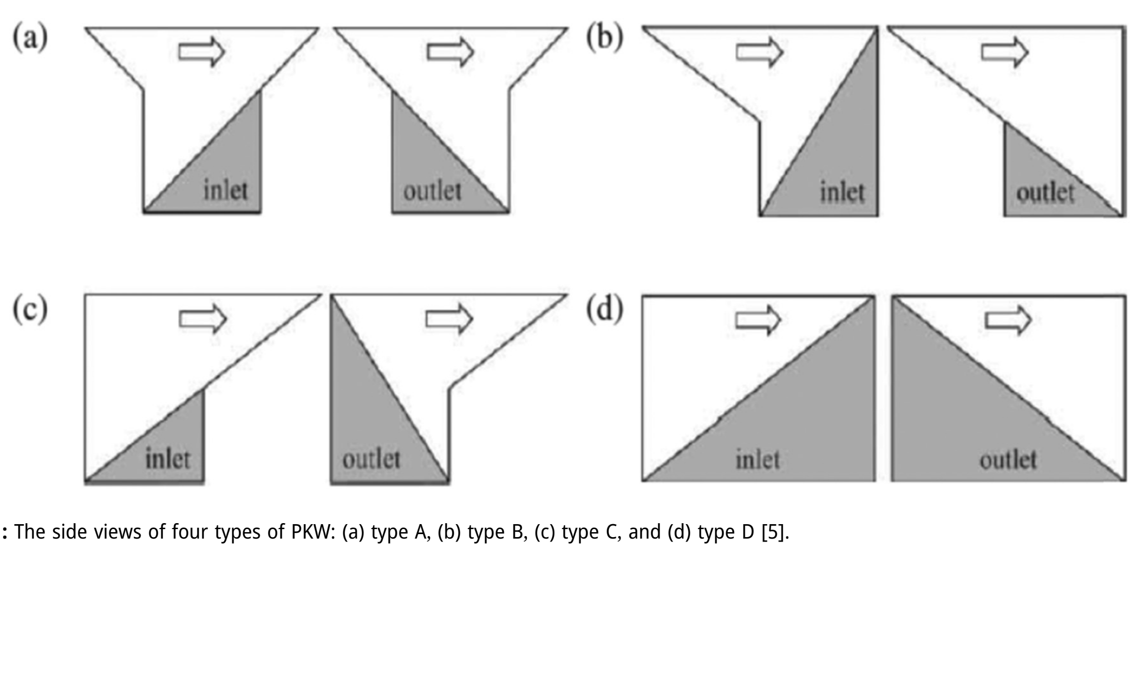

Figure 1: The side views of four types of PKW: (a) type A, (b) type B, (c) type C, and (d) type D [5].

and discharge capacity of four PKSWs type B with various crest length-to-width ratios (L/W).

2 CFD modeling with Flow-3D software

This research solved the CFD problem using the Flow-3D software. With Flow-3D, engineers can view a variety of physical flow processes like microfluidics, hydropower, infrastructures, waves at sea, and many other industrial challenges. Therefore Flow-3D is a powerful and efficient simulation tool for CFD technology. Partial differential equations embody the conservation laws of momentum, energy, and mass govern fluid movement. These equations can be combined to form the Navier–Stoke equations [14]. A single nested mesh block, neighboring linked mesh blocks, or a combination of nested and linked mesh blocks can be used with Flow-3D, which uses an orthogonal coordinate system rather than a body-fitted one. Also, to locate obstacles, Flow-3D uses both a Fractional Area/Volume Obstacle Representation approach and the Volume of Fluid (VOF) method [15] to determine the position of the free surface. The solutions from the numerical models in Flow-3D are typically used as checkpoints or physical model experiments before being used in real settings or calibrated using contrasts with field data [16].

3 Flow theory

The physical characteristics of this study take into account an incompressible, viscous fluid, with both the continuity and the momentum equations acting as the study's governing equations. In the three-dimensional Cartesian (x, y, z) system, Flow-3D numerically solves the Navier–Stokes equations as a function of time (t) for the velocity components (u, v, w) and pressure in both compressible and incompressible forms [15]. The expressions of Naiver–stokes equations for the preservation of the mass continuity and momentum equations for this study with constant viscosity and density are, respectively, as follows [17]:

$$\frac{\partial u}{\partial x} + \frac{\partial v}{\partial y} + \frac{\partial w}{\partial z} = 0, \tag{1}$$

$$\rho g_x - \frac{\partial P}{\partial x} + \mu\left(\frac{\partial^2 u}{\partial x^2} + \frac{\partial^2 u}{\partial y^2} + \frac{\partial^2 u}{\partial z^2}\right) = \rho\frac{\partial u}{\partial t}, \tag{2}$$

$$\rho g_y - \frac{\partial P}{\partial y} + \mu\left(\frac{\partial^2 v}{\partial x^2} + \frac{\partial^2 v}{\partial y^2} + \frac{\partial^2 v}{\partial z^2}\right) = \rho\frac{\partial v}{\partial t}, \tag{3}$$

$$\rho g_z - \frac{\partial P}{\partial z} + \mu\left(\frac{\partial^2 w}{\partial x^2} + \frac{\partial^2 w}{\partial y^2} + \frac{\partial^2 w}{\partial z^2}\right) = \rho\frac{\partial w}{\partial t}, \tag{4}$$

where μ is the coefficient of viscosity, ρ is the density of the fluid, P is the pressure, g_i is the gravity in the Cartesian (x, y, z) system, (u, v, w) are the components of velocity in (x, y, z) Cartesian system, and t is the time.

4 Description of PKSW models

To confirm the effectiveness and predictability of the current numerical study, four models of PKSW type B are simulated in Flow-3D software, to investigate the effect of L/W parameter on the discharge coefficient of PKSW in this study. The PKSW models were designed within a 2.5 mm

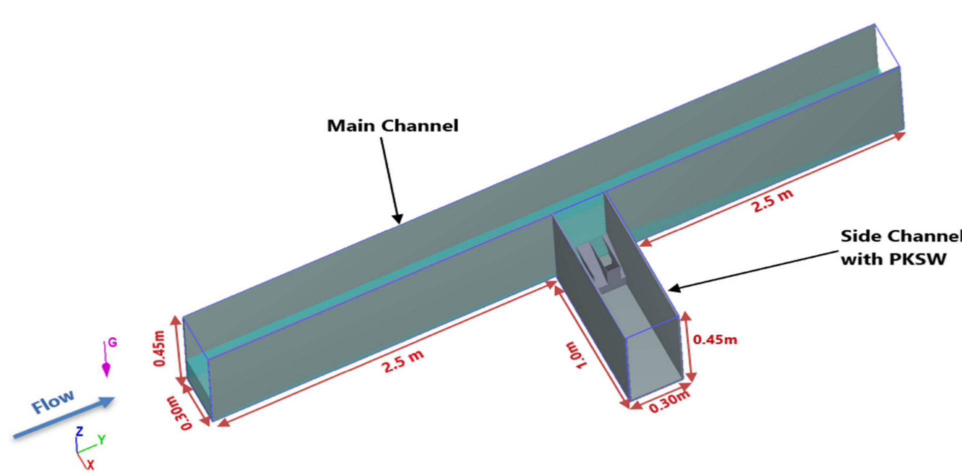

Figure 3: The 3D sketch of the work section of the channel.

thickness of sidewall boundary using 3D drawings and formed the flat top crest on all edges. The main study channel was rectangular flume of 15 m length, 0.30 m width in the cross-section, and 0.45 m height [3]. The work section of the simulation is shown in Figure 3.

Table 1 clarifies the geometric properties of the model, flow characteristics, and the fluid properties.

The geometrical parameters of PKSW models used in simulation, are represented in Table 2.

Figure 4 shows the details of variables of PKSW type B model of this study in 3D view.

5 Numerical simulations set-up

By using the Flow-3D program, the CFD problem was solved. As a numerical method for locating and tracking the fluid's free surface, this software uses the VOF method to simulate the flow phenomenon. A computational grid is created by separating the domain of the solution into cells, introducing a fractional volume function, which has a value of unity in cells that are full of fluid, zero in cells that are empty, and a value between 1 and 0 in cells that have a fluid-free surface [15].

Table 1: Variables considered in the current study

Variables	Definition
B	Length upstream-downstream of the PKSW, for type B: $B = B_b + B_o$
B_b	The base length
B_i	Downstream overhang length (inlet key)
B_o	Upstream overhang length (outlet key)
W	Total width of PKSW
W_i	The width of the inlet key
W_o	The width of the outlet key
P	PKSW height
P_d	Height of dam
L	Total developed crest length of PKSW
T_s	The thickness of the sidewall
Q	Discharge at the main channel prior to the beginning of the PKSW (m^3/s)
Q_1	The total discharge into the main channel at the upstream end of PKSW
Q_2	The total discharge into the main channel at the downstream end of PKSW
Q_w	Outflow discharge from PKSW
g	The acceleration of gravity
C_{PW}	Discharge coefficient of the PKSW
h_1	Head of piezometric over the side weir at the upstream end
h_2	Head of piezometric over the side weir at the downstream end
h_a	An average head of piezometric over the side weir
ρ	The mass density of water
μ	The dynamic viscosity of water
σ	Surface tension of water

Table 2: Geometrical Parameters and dimensions (in cm) of the PKSW models

Model	B	P	Pd	L/W	W_i/W_o	B/P	B_o/B	Pd/P
B1	22	9	5.4	4	1	2.4	0.5	0.6
B2	15.5	6.5	3.9	3	1	2.4	0.5	0.6
B3	30	12.5	7.5	5	1	2.4	0.5	0.6
B4	37	15.4	9.2	6	1	2.4	0.5	0.6

For the simulation, only one fluid (water) was chosen, and a free surface or sharp interface was specified. 25 s was chosen as the finish time for all simulations for the models. Moreover, all simulations used the fluid characteristics at 20°C with SI units. In addition, the (k–e) turbulent model is the most popular choice since it is simple to solve, converges rather rapidly, and is based on recommendations in Flow Science [14]. All simulations were represented in three dimensions, so that this study used two mesh blocks, one for main channel and the other for the side channel with the model of PKSW. Starting with a relatively big mesh and gradually reducing it until the desired output no longer varies significantly with subsequent mesh size reductions is an efficient technique to discover the decisive mesh size, as shown in Figure 5.

One of the key components in the development and success of the simulation process was the cubic shape of the mesh cells in the blocks of Flow-3D software because

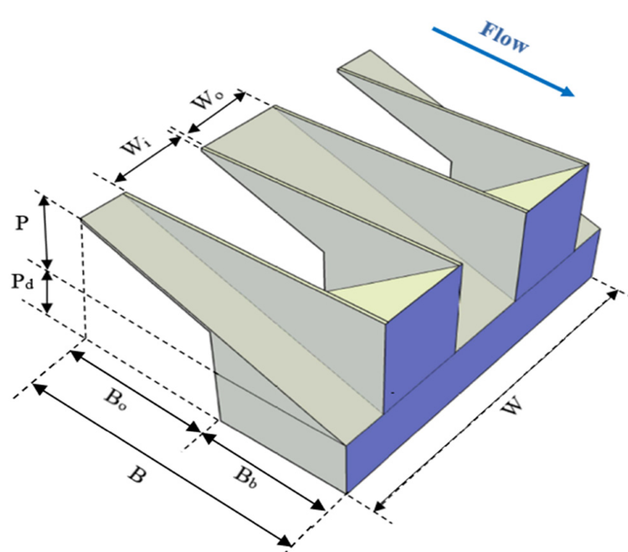

Figure 4: Sketch of PKSW model type B (3D view).

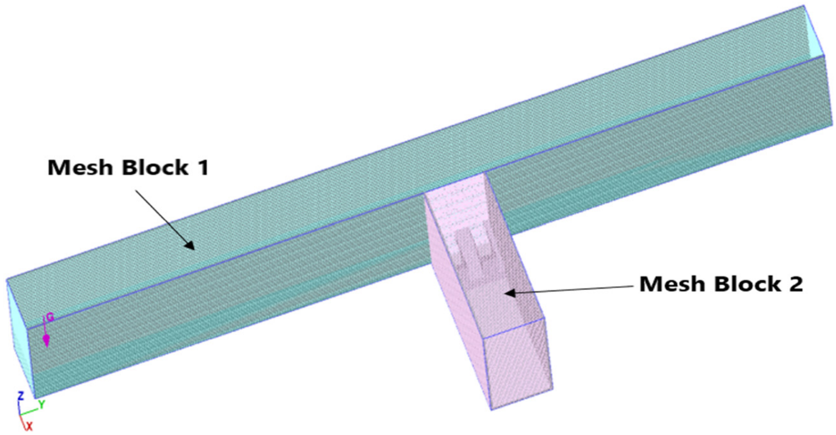

Figure 5: Mesh arrangement used in PKSW modeling.

mesh and cell size are fundamental elements of any simulation of a numerical model [18]. Therefore, in the present study, the mesh cells were selected as total cells for the mesh blocks to determine which cell size satisfies the phenomenon requirements of flowing in the PKSW. The total number of cells used in this study to best represent each of the PKSW models ranged between 700,000 and 1,600,000 as an option for the total number of cells. Figure 6 represents the comparison of the sensitivity of the total number of cells that it used.

While boundary conditions include three axes (*X*, *Y*, and *Z*), and each axis has Min. and Max. values. In the current study, the *X*-direction denotes the channel's length, the *Y*-direction denotes its width, the *Z*-direction denotes its height, and the origin point is located at the start of the upstream channels. 25 s is the finish time used to reach the

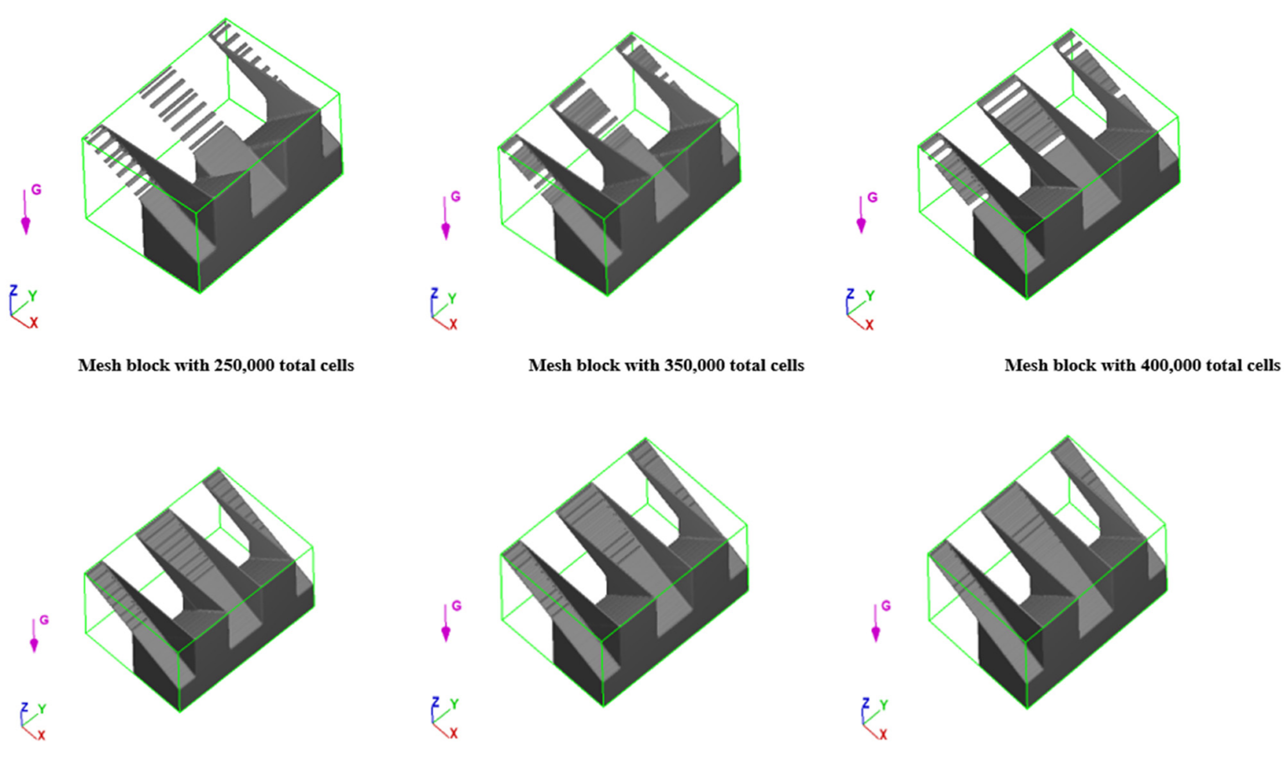

Figure 6: Appreciation of mesh sensitivity to the total cells used in the PKSW model.

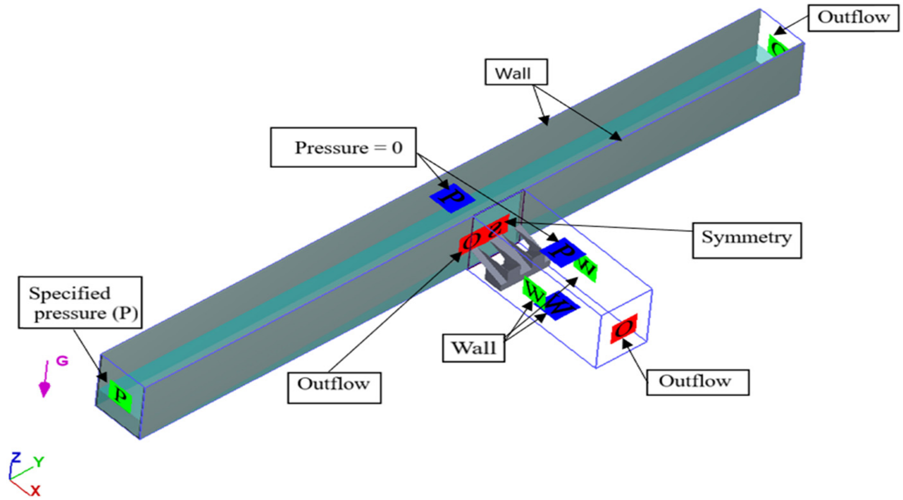

Figure 7: The applied boundary conditions for PKSW modeling.

steady-state condition. Figure 7 shows the configuration of the boundary conditions selected.

6 Verification model

One of the main aims of this research is the verification between numerical and experimental results, and utilizing the data from the experiments that are offered by Karimi et al. [7], the numerical simulation was verified, through CFD modeling of the PKSW by the Flow-3D software. In the research chosen, the type of the PKSW is rectangular (RPKSW) type C and placed in the side channel that was orthogonal to the main channel. The dimensions of the tested PKSW are listed in Table 3. To achieve successful outcomes in a numerical simulation of the laboratory model, a two-mesh block format was used, with the cell size in the range of 0.001–0.002 mm in the two-mesh, and a time of 25 s required to reach a steady state. The time needed to obtain the results is 5 days.

The boundary condition shown in Figure 8 was applied in this simulation, while Figure 9 shows the results of the flow pattern on the tested PKSW of the verification study.

After a comparison between experimental data and numerical results from Flow-3D using the range of the

Table 3: Dimensions of the tested PKSW [7]

Model	P (cm)	B (cm)	B_b (cm)	B_i (cm)	P_d (cm)	L/W
M1	5	16	8	8	0	2

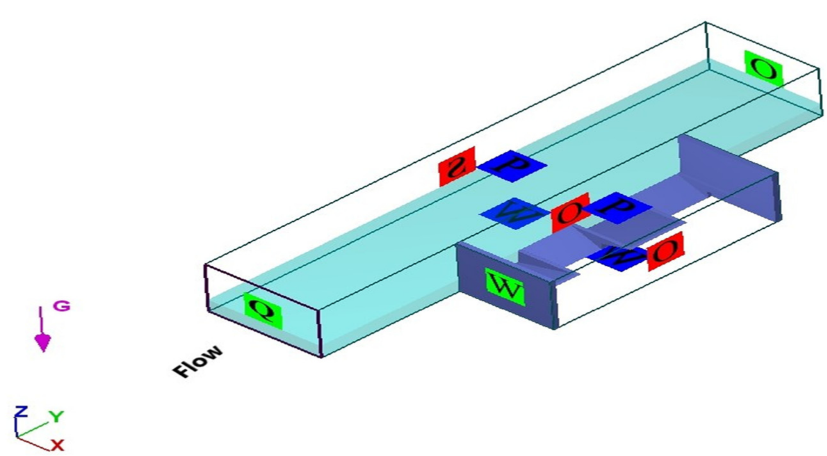

Figure 8: The boundary condition applied in the PKSW of the verification study.

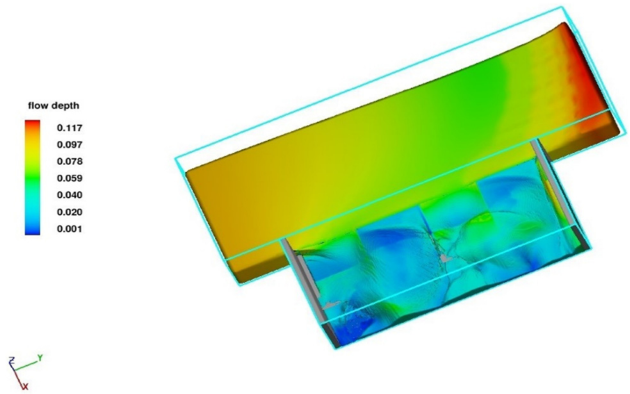

Figure 9: The flow pattern on the tested PKSW of the verification study.

discharge coefficients, calculation of the difference between the results has been made by the Mean Absolute Relative Error (MARE) stated in equation (5).

$$\text{MARE} = \frac{C_{\text{Mexperimental}} - C_{\text{Mnumerical}}}{C_{\text{Mexperimental}}}. \quad (5)$$

The results of both the numerical and experimental tests shows a significant level of agreement with a range of about 9.54–5.25%, as shown in Figure 10.

7 The results of Flow-3D

The Flow-3D program was used in this study to run 20 simulation instances for 4 PKSWs with different L/W ratios (L/W = 3, 4, 5, and 6). As a consequence, depending on the chosen physics, number of cells, modeling time, etc., the time needed to obtain the results of the present research is approximately 1–3 days. Figures 11–14 show the flow over the PKSWs with different L/W ratios.

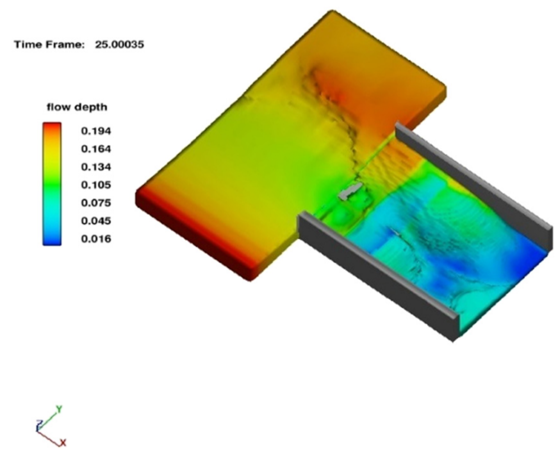

Figure 11: The flow over PKSW model (B2 with L/W = 3).

8 Measurement of the discharge coefficient

Due to the spatially variable flow at the side weir, the flow conditions in the main channel are spatially variable flow with decreasing discharge [12]. As a function of weir length (q), the equation for the discharge flowing over the side weir is written as follows:

$$q = -\left(\frac{\mathrm{d}Q}{\mathrm{d}x}\right) = \left(\frac{\mathrm{d}Q_{\mathrm{w}}}{\mathrm{d}x}\right) = \frac{2}{3}C_{\mathrm{d}}\sqrt{2g}\,(y_1 - P)^{1.5}, \quad (6)$$

where Q is the discharge of the main channel, x is the distance from the starting of the side weir, Q_{w} is the

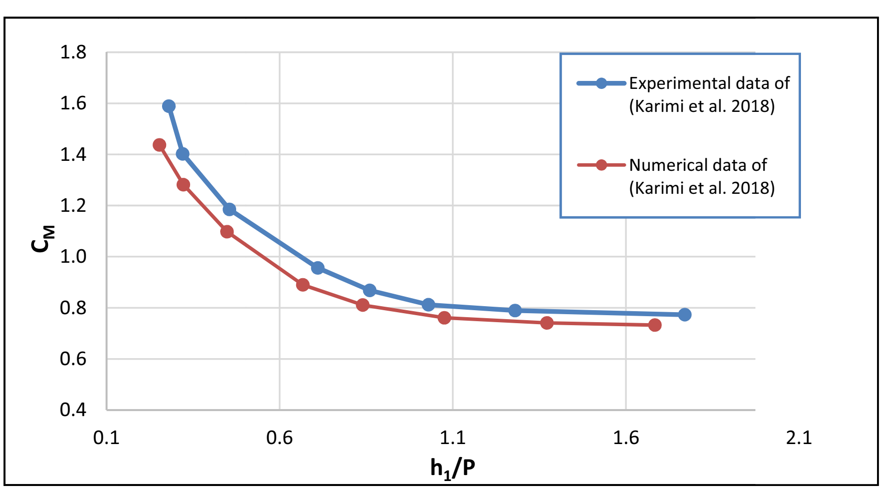

Figure 10: Results of the comparison of discharge coefficient between experimental and numerical data of the verification study.

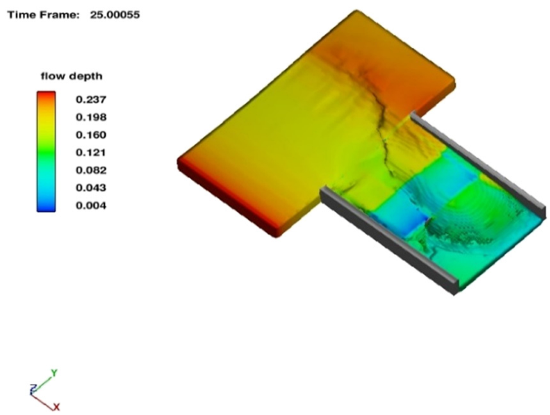

Figure 12: The flow over PKSW model (B1 with *L*/*W* = 4).

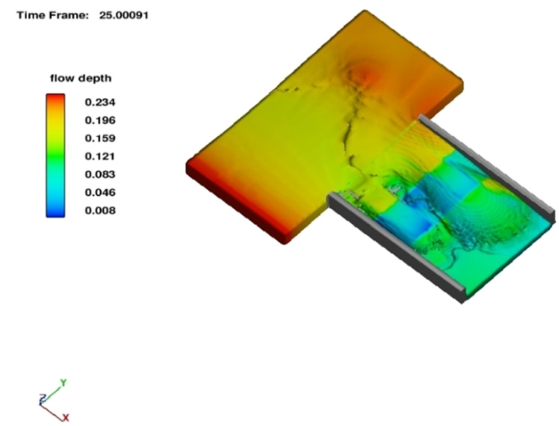

Figure 13: The flow over PKSW model (B3 with *L*/*W* = 5).

discharge over the side weir, C_d is the main discharge coefficient, g is the acceleration of gravity, y_1 is the depth of flow at the upstream end of the side weir, P is the height of side weir, and $(y_1 - P)$ represents the head of piezometric over the side weir.

By using Schmidt's method [19], which is satisfied when the flow rate in the river regime has been reached and sustained, the discharge coefficient for the current study was calculated and assigned by the abbreviation C_{PW}.

$$Q_w = C_{\mathrm{PW}} \frac{2}{3} \sqrt{2g}\, W h_a^{1.5}, \tag{7}$$

$$h_a = \frac{1}{2}(h_1 + h_2), \tag{8}$$

where W is the total width of PKSW, h_a is defined as an average head of piezometric over the side weir, h_1 is the head of piezometric over the weir at the upstream end, and

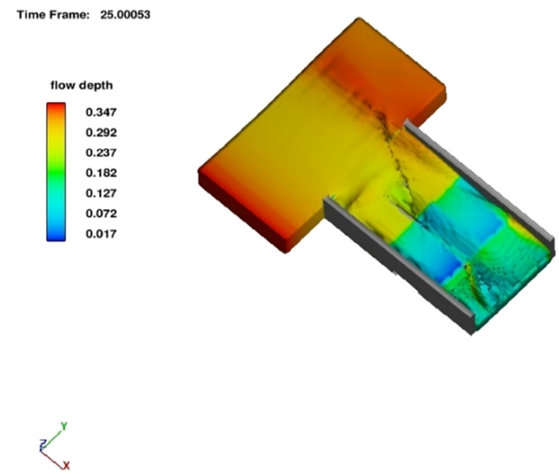

Figure 14: The flow over PKSW model (B4 with *L*/*W* = 6).

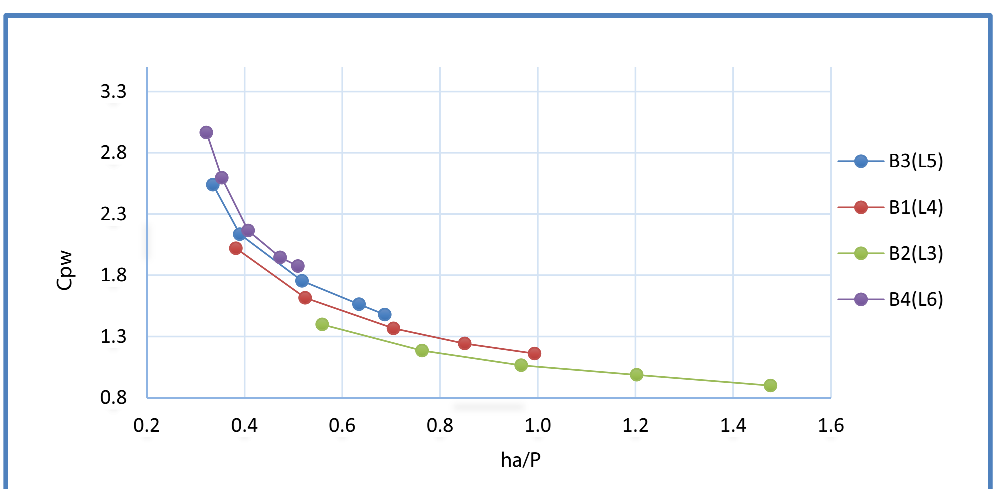

Figure 15: The variation in C_{pw} discharge coefficient vs h_a/P for different *L*/*W* ratios of the PKSW type B.

h_2 is the head of piezometric over the weir at the downstream end.

9 Effect of the hydraulic parameter (h_a/P)

After completing the numerical tests and analyzing them to obtain the basic objectives of this research, the data generated from the Flow-3D software were analyzed on the four models of the PKSW type B and at several discharges (starting from about 30–45 l/s) in the main channel during free flow conditions. In this study, the great importance of the factor h_a/P was taken into account in the discharge above the PKSW, and its importance comes from the fact that it represents the upstream head above the crest of the side weir. It is clear from the data in Figure 15 that increasing the head over the side weir has negative effects on the discharge coefficient (C_{pw}). The behavior of the flow through the inlet, outlet, and side crests may provide an explanation for this. The ratio h_a/P is measured in a range of around (0.322–1.477). In the vicinity of low h_a/P values, roughly between 0.3 and 0.75, it appears that the discharge coefficient is reduced more quickly. The reduction becomes moderately reduced after this range. This suggests that only when h_a/P is in the lower range (about less than 0.75), the geometrical characteristics may raise or reduce the discharge capacity significantly.

10 Effect of the crest length to the width of the PKSW (L/W)

In this research, four models of PKSW were tested with different ratios of crest length to the width of the PKSW (L/W), and it was shown by reviewing the results that L/W is a very important factor affecting the discharge coefficient. Figure 15 shows the results of the analysis of the four models, namely, B1(L/W = 4), B2(L/W = 3), B3(L/W = 5), and B4(L/W = 6).

The ratio L/W = 5, which fulfills the geometry proposed by Lempérière et al. [4], is used to determine the percentage change of C_{pw} for this group of models in comparison to model B3. The data are in various h_a/P ranges, as seen. Their various heights (P) provide an explanation for this. Figure 16 shows the relationship between the C_{pw} and the head (h_a).

After the comparison of the C_{pw} of different models, the results as shown in Figure 15, the model B4 with L/W = 6 has the highest range of the discharge coefficient and is more efficient than model B3 (L/W = 5) by about 17–27%. While model B1 (L/W = 4) is less efficient than model B3 by about 20–22%. Also, model B2 (L/W = 3) is lesser in capacity compared with model B3 by about 45%. The L/W ratio had to be increased for type B and impacts only the low head ratio; therefore, when the head rises, there is increased submergence at the outlet key, which reduces the side weir performance [20].

Finally, it should be clear that L/W has a significant impact on the PKSW discharge capacity, which can increase to a maximum level if L/W is increased while the other parameters remain the same and the ratio (h_a/P) is maintained at

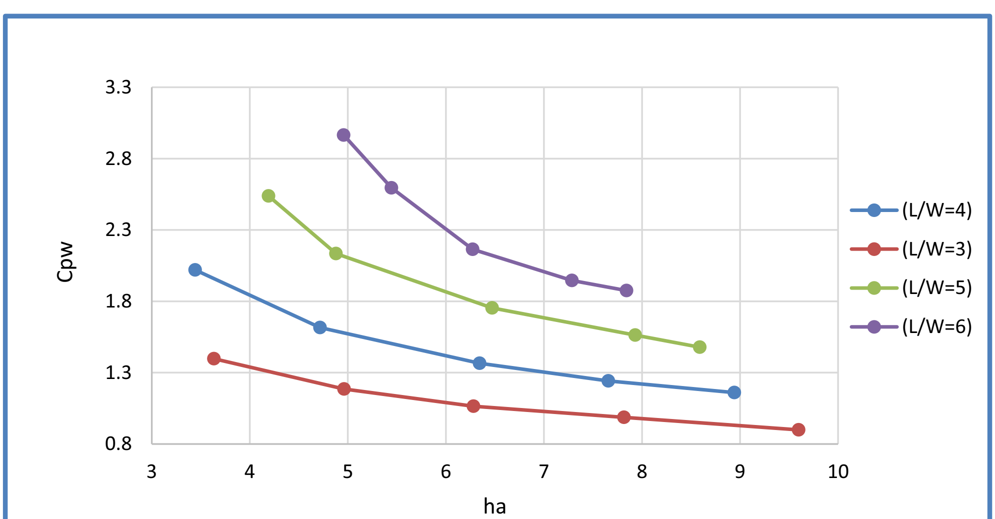

Figure 16: The relationship between the C_{pw} and the head (h_a) for different L/W ratios of PKSW.

or below 0.75. This is due to an increase in the flow path of the PKSW, and this behavior is comparable to that of frontal configurations of piano keys and labyrinth weirs [7].

11 Conclusion

Since the CFD methodology was applied, Flow-3D's capacity to represent the flow over the side weir has improved. This was found by numerically simulating the behavior of the flow rate going over the PKSW using settings in the Flow-3D software. In this research, numerical studies have been performed on four models of PKSW type B with different ratios of the crest length to the width (L/W) of PKSW, to determine the discharge coefficient. These ratios are $L/W = 3$, 4, 5, and 6.

The important results that could be obtained through this study are as follows:

1. As a conclusion to the current study, it can be observed that L/W has a significant impact on the PKSW discharge capacity and can increase to a maximum level when all other parameters are held constant, this is caused by an increase in the PKSW's flow path.
2. When comparing the model ($L/W = 5$) to the other models, it was noted that the discharge coefficient was highest when ($L/W = 6$), because its efficiency was higher by about (17–27%).
3. The two models $L/W = 4$ and $L/W = 3$ are lower by about (20–22%) and 45%, respectively.
4. The effect of h_a/P on the coefficient of discharge was also noted, it was found that increasing the h_a/P negatively affects the coefficient of discharge.
5. In order to obtain a high capacity for the discharge coefficient, the ratio (h_a/P) is smaller than 0.75 or between the range ($0.3 \le h_a/P < 0.75$).

Conflict of interest: The authors declare that they have no conflict of interest.

Data availability statement: Most datasets generated and analyzed in this study are comprised in this submitted manuscript. The other datasets are available on reasonable request from the corresponding author with the attached information.

References

[1] Anderson RM, Tullis BP. Piano key weir hydraulics and labyrinth weir comparison. J Irrig Drain Eng. 2013;139(3):246–53.

[2] Khassaf SI, Al-Baghdadi MB. Experimental study of non-rectangular piano key weir discharge coefficient. Int J Energy Environ. 2015;6(5):425.

[3] Al-Baghdadi MB. Study of the Hydraulic Performance of Flow over Piano Key Weir. M.Sc. Thesis Submitted to the Hydraulic Structures, Civil Engineering, Faculty of Engineering, University of Kufa, 2015.

[4] Lempérière F, Vigny J-P, Ouamane A. General comments on labyrinths and piano key weirs: The past and present. Proceedings of the International Conference Labyrinth and Piano Key Weirs – PKW, Liège, Belgium. London: CRC Press; 2011. p. 17–24.

[5] Ribeiro ML, Pfister M, Schleiss AJ, Boillat JL. Hydraulic design of A-type piano key weirs. J Hydraul Res. 2012;50(4):400–8.

[6] Pralong J, Vermeulen J, Blancher B, Laugier F, Erpicum S, MacHiels O, et al. A naming convention for the piano key weirs geometrical parameters. Labyrinth and Piano Key Weirs - Proceedings of the International Conference on Labyrinth and Piano Key Weirs, PKW. CRC Press; 2011. p. 271–8.

[7] Karimi M, Attari J, Saneie M, Reza M, Ghazizadeh J. Side weir flow characteristics: Comparison of piano key, labyrinth, and linear types. J Hydraul Eng. 2018;144(12):1–13.

[8] Mehri Y, Soltani J, Saneie M, Rostami M. Discharge coefficient of a C-type piano key side weir at 30° and 120° sections of a curved channel. Civ Eng J. 2018;4(7):1702.

[9] Seyedjavad M, Naeeni STO, Saneie M. Laboratory investigation on discharge coefficient of trapezoidal piano key side weirs. Civ Eng J. 2019;5(6):1327–40.

[10] Saghari A, Hosseini K, Saneie M. Experimental study of trapezoidal piano key side weirs in a curved channel. Flow Meas Instrum. 2019;70:101640.

[11] Karimi M, Jalili Ghazizadeh M, Saneie M, Attari J. Experimental and numerical study of a piano key side weir with oblique keys. Water Environ J. 2020;34(S1):444–53.

[12] Mehri Y, Esmaeili S, Soltani J. Experimental study and performance comparison on various types of rectangular piano key side weirs at a 120° section of a 180° curved channel. Appl Water Sci. 2020;10:1–10.

[13] Kilic Z, Emiroglu E. Study of hydraulic characteristics of trapezoidal piano key side weir using different approaches. Water Supply. 2022;22(8):6672–91.

[14] Flow Science. FLOW-3D version 11.0.4 User Manual. 2015. [cited 2023 May 10]. Available from FLOW-3D user's, https://flowsciences.com.

[15] Hirt CW, Nichols BD. Volume of fluid (VOF) method for the dynamics of free boundaries. J Comput Phys. 1981;39(1):201–25.

[16] Chanel PG. 'An evaluation of computational fluid dynamics for spillway modeling'. MSc Thesis. Winnipeg, Manitoba, Canada: University of Manitoba; 2008.

[17] White FM. University of Rhode Island Boston. 4th Edition. 1998.

[18] Al-Shaikhli H, Khassaf S. Stepped mound breakwater simulation by using flow 3D. Eurasian J Eng Technol. 2022;6(2795–7640):60–8.

[19] Ikinciogullari E, Emiroglu EM. Estimation of triangular labyrinth side weir discharge capacity using schmidt approach. Sigma J Eng Nat Sci. 2019;37(1):289–303. https://www.researchgate.net/publication/333088943.

[20] Khassaf SI, Jawad LA, Elkatib ZA. Hydraulic behavior of piano key weir type B under free flow conditions. Int J Sci Technol Res. 2016;5:158–63. www.ijstr.org.